Mol Genet Genomics
DOI 10.1007/s00438-016-1168-1

ORIGINAL ARTICLE

Genome-wide identification, classification and expression analysis in fungal–plant interactions of cutinase gene family and functional analysis of a putative *ClCUT7* in *Curvularia lunata*

Tong Liu[1,2] · Jumei Hou[1] · Yuying Wang[1] · Yazhong Jin[1] · Wayne Borth[2] · Fengzhou Zhao[1] · Zheng Liu[1] · John Hu[2] · Yuhu Zuo[1]

Received: 12 July 2015 / Accepted: 6 January 2016

Abstract Cutinase is described as playing various roles in fungal–plant pathogen interactions, such as eliciting host-derived signals, fungal spore attachment and carbon acquisition during saprophytic growth. However, the characteristics of the cutinase genes, their expression in compatible interactions and their roles in pathogenesis have not been reported in *Curvularia lunata*, an important leaf spot pathogen of maize in China. Therefore, a cutinase gene family analysis could have profound significance. In this study, we identified 13 cutinase genes (*ClCUT1* to *ClCUT13*) in the *C. lunata* genome. Multiple sequence alignment showed that most fungal cutinase proteins had one highly conserved GYSQG motif and a similar DxVCxG[ST]-[LIVMF](3)-x(3)H motif. Gene structure analyses of the cutinases revealed a complex intron–exon pattern with differences in the position and number of introns and exons. Based on phylogenetic relationship analysis, *C. lunata* cutinases and 78 known cutinase proteins from other fungi were classified into four groups with subgroups, but the *C. lunata* cutinases clustered in only three of the four groups. Motif analyses showed that each group of cutinases from *C. lunata* had a common motif. Real-time PCR indicated that transcript levels of the cutinase genes in a compatible interaction between pathogen and host had varied expression patterns. Interestingly, the transcript levels of *ClCUT7* gradually increased during early pathogenesis with the most significant up-regulation at 3 h post-inoculation. When *ClCUT7* was deleted, pathogenicity of the mutant decreased on unwounded maize (*Zea mays*) leaves. On wounded maize leaves, however, the mutant caused symptoms similar to the wild-type strain. Moreover, the *ClCUT7* mutant had an approximately 10 % reduction in growth rate when cutin was the sole carbon source. In conclusion, we identified and characterized the cutinase family genes of *C. lunata*, analyzed their expression patterns in a compatible host–pathogen interaction, and explored the role of *ClCUT7* in pathogenicity. This work will increase our understanding of cutinase genes in other fungal–plant pathogens.

Keywords Cutinase · Compatible interaction · Expression patterns · Pathogenicity

Communicated by S. Hohmann.

Electronic supplementary material The online version of this article (doi:10.1007/s00438-016-1168-1) contains supplementary material, which is available to authorized users.

✉ Tong Liu
liutongamy@sina.com

✉ Yuhu Zuo
zuoyhu@163.com

[1] Institute of Applied Microbiology and Plant Pathogenic Fungi, Agricultural College, Heilongjiang Bayi Agricultural University, Daqing 163319, Heilongjiang, People's Republic of China

[2] Department of Plant and Environmental Protection Sciences, University of Hawaii, 3190 Maile Way, Honolulu, HI 96822, USA

Introduction

The cuticle is the outermost layer of the aerial part of all plants and forms the first obstacle to invasion by plant pathogens. However, most plant pathogens produce cutinases that catalyze the degradation of the cuticle and promote penetration by the pathogen. Degradation of the host plant cuticle at the inoculation site leads to successful penetration and infection by various pathogens (Maddock 1979;

Shaykh et al. 1977). Moreover, if the cutinase activity of a fungal–plant pathogen is deleted, its pathogenicity is often weakened (Davies et al. 2000; Zhang et al. 2005) or eliminated (Dickman and Patil 1986; Stahl and Schafer 1992; Stahl et al. 1994).

Curvularia leaf spot of maize (*Zea mays*) caused by *Curvularia lunata* (Wakker) Boed was one of the most severe diseases in China's maize (corn) production zone during the 1990s and is still prevalent nationwide (Dai et al. 1995, 1998; Gao et al. 2014a, b; Ito et al.1979; Li et al. 2006; Macri and Lenna 1974). The fungus causes water-soaked or necrotic spots with yellow halos on leaves (Hou et al. 2013). It is presumed that this pathogen produces a series of degradation enzymes that soften the cell wall and breach the host's defenses. Although some degradation enzymes such as polygalacturonase, polymethylgalacturonase, cellulases and laccases also have important roles in colonization by the pathogen (Feng et al. 2002; Zhou et al. 2010), little is known about the characteristics of the cutinase genes, their expression, or their roles in the pathogenesis of *C. lunata.* Therefore, an investigation of the cutinase genes in *C. lunata* is important and timely.

The recent completion of a draft genome of *C. lunata* provided information to help identify the cutinase genes of this fungus (Gao et al. 2014a, b). In this study, we identified 13 cutinase genes in *C. lunata*, and analyzed the structures of their encoded proteins, gene intron–exon distributions, phylogenetic relationships, motif distributions, and their expression patterns in a compatible host–pathogen interaction. We also characterized the function of an up-regulated cutinase gene, *ClCUT7*, in the penetration process. The results of these analyses suggested that the cutinases of *C. lunata* are involved in its pathogenesis on maize. These results will lead to future systematic analyses of the functions of the cutinase genes in this plant pathogen.

Materials and methods

Fungal strains and plant material

The highly virulent strain CX-3 of *C. lunata*, provided by Prof. Jie Chen (Shanghai Jiaotong University, Shanghai, China) was used as the wild-type strain. The maize inbred line 'Huangzao 4′ was used as the susceptible host plant. Maize seeds were surface sterilized in 10 % sodium hypochlorite for 5 min, rinsed with sterile water, and germinated on wet filter paper for 2 days at 25 °C. Germinated seeds were transferred to 14 × 18-cm pots and kept in a growth chamber for 4 weeks at 25 °C with a 14 h photoperiod and 60 % relative humidity.

Cutinase sequence search

Data for the *C. lunata* genome were downloaded from http://www.ncbi.nlm.nih.gov/nuccore/JFHG00000000. Pedicted protein databases were constructed using BioEdit® software. The keyword "cutinase" was used to search the National Center for Biotechnology Information (NCBI) protein database. The known cutinase proteins from plant pathogens were downloaded (Additional file 1) as queries against the predicted protein databases from *C. lunata*. Proteins with a significant *E*-value ($<1.0^{-10}$) were extracted from the predicted protein database of *C. lunata* and redundant protein sequences were discarded. The candidate proteins were analyzed using the conserved domain database (CDD) server at NCBI. The proteins containing cutinase domains were used for further analyses.

Sequence analysis

The molecular weights (kDa) and isoelectric points (PI) of each predicted cutinase protein were calculated using online ExPASy programs (http://www.expasy.org/tools/). Multiple alignments were made with the Clustal W2 program (http://www.ebi.ac.uk/Tools/msa/clustalw2/) and GENEDOC v. 2.7000© software. Amino acid sequences used for conserved residues analysis were as indicated (Additional file 2). All predicted cutinase protein sequences from *C. lunata*, plus 78 other known cutinase amino acid sequences (Additional file 3) downloaded from the NCBI database, were aligned for phylogenetic analyses with MEGA6.0© (http://megasoftware.net) using the neighbor-joining method (minimum evolution criterion; bootstrap values performed on 1000 replicates) (Staitou and Nei 1987). To reveal the exon–intron organization of the cutinase genes in *C. lunata*, we aligned the genomic and cDNA sequences using Clustal W2 (http://www.ebi.ac.uk/Tools/msa/clustalw2/). Structural analyses of the cutinase genes were performed using the online server GSDS (http://gsds.cbi.pku.edu.cn/). Conserved motifs were identified using the online MEME analysis tool (http://meme.nbcr.net/meme/cgi-bin/meme.cgi) with the following parameters: optimum motif width ≥6 and ≤200; maximum number of motifs = 25.

Sample preparation, RNA isolation and cDNA synthesis

To analyze the transcript levels of cutinase genes during host–pathogen interactions, maize plants at the seven-leaf stage were inoculated using an air sprayer with 1×10^6 conidia/ml suspensions of *C. lunata* CX-3 in 2 % sucrose and 0.02 % Tween 20 as described (Huang et al. 2008). Control plants were sprayed with sucrose and Tween 20 only. Maize leaves were collected at 0, 0.5, 1.5, 3 and 24 h

post-inoculation (hpi). All samples were immediately frozen in liquid nitrogen and stored at −80 °C until RNA isolation. Total RNAs were extracted using a QIAGEN RNeasy Plant® Kit (Beijing, China) following the manufacturer's recommendations. RNA concentrations were measured on a NanoDrop® spectrophotometer (ND-1000) and quality was checked by agarose gel electrophoresis (28SrRNA/18Sr RNA ratios). We synthesized cDNA from the total RNAs (0.5–1 mg) using an MMLV reverse transcriptase cDNA Synthesis Kit® following the manufacturer's instructions (Cat#D6130, TaKaRa, Tokyo, Japan).

Quantitative PCR

Quantitative RT-PCR (qRT-PCR) was performed in 20-ml reaction volumes using Super-Real PreMixPlus® (SYBR-Green; Cat. # FP205, Tiangen Biotech, Beijing, China) on an ABI PRISM7500 sequence-detection system according to manufacturer's instructions. *GAPDH* was used as the internal control. We used the comparative C_t method ($\Delta\Delta C_t$) to calculate relative expression levels. Statistical analysis of gene expression was conducted using ANOVA (SAS 8.2). The primer pairs used for qRT-PCR are listed in Additional file 4. The experiments were repeated at least twice.

Deletion of the *ClCUT7* gene

Nucleotide sequences from 3000 bp upstream and 2500 bp downstream of the *ClCUT7* gene were identified from the *C. lunata* genome. We constructed a gene deletion cassette using a double-joint PCR technique (DJ-PCR) (Yu et al. 2004). A deletion cassette containing flanking sequences of the *ClCUT7* gene and a selectable marker hygromycin phosphotransferase (*hph*) gene was amplified by three sequential cycles of PCR. In the first cycle, the two flanking fragments of *ClCUT7* and *hph* with the TrpC promoter of *Aspergillus nidulans* (HPH), were amplified with primers cu1 s/cu1a, cu2 s/cu2a and hphs/hpha (Additional file 5), respectively. In the second cycle, two fusion fragments were amplified using the first-round PCR products as templates. In the third PCR cycle, the deletion cassette was developed with primers cu1s and cu2a using 100-fold dilutions of the two fusion fragments as templates from the second round of PCR. The deletion cassette products were introduced into protoplasts of wild-type strain CX-3 as described (Liu et al. 2010). Hygromycin-resistant transformants were isolated and screened for durable resistance by growing them for six consecutive transfers on potato dextrose agar (PDA) containing 250 μg ml^{-1} hygromycin. DNA from the hygromycin-resistant transformants was extracted as described previously (Liu et al. 2011) and used to detect the gene deletion mutants. The resulting mutants were confirmed by Southern blot analysis and RT-PCR. The probe used for Southern blotting was amplified with primers cus and cua, and labeled with biotin. Southern blotting was performed as described (Liu et al. 2011). Primers used for construction of the deletion cassette, the initial detection of the gene deletion mutant and RT-PCR are listed in Additional file 5, Table S5.

Colony characteristics and pathogenicity assay

Mycelium from *C. lunata* (wild-type strain CX-3) and the *ClCUT7* deletion mutant were inoculated onto plates containing PDA and incubated for 7 days at 25 °C. Colony morphology was documented with a Nikon D3200 DSLR camera. To measure vegetative growth, a 4-mm mycelial plug from each strain was transferred to fresh PDA plates and incubated in the dark for 7 days at 25 °C. Colony diameters were measured and recorded daily. Vegetative growth was based on the change in colony diameter after 7 days. Each experiment was performed three times. Conidia production was determined by inoculating both wild-type and mutant strains onto PDA plates and incubating them for 12 days at 25 °C in darkness. Then 10 ml of sterile distilled H_2O was added to each plate, the conidia dislodged with a sterile swab, and then counted using a hemocytometer. Conidial morphology was observed and photographed using an Olympus BX51 microscope (Olympus, Center Valley, PA, USA). To observe appressorium formation, conidia were inoculated onto cellophane disks placed on PDA, examined microscopically after 6, 9, and 12 h, and photographed using Olympus cellSens® standard software. For pathogenicity assays, we removed the fourth leaf of maize cultivar Huang Zao 4 at the seventh leaf stage, cut it into 5-cm fragments, and placed the fragments on moist filter paper in humid petri dishes at 25 °C. Wounded and unwounded leaves were inoculated with a suspension of 1×10^6 conidia/ml in 0.02 % Tween 20 as previously described (Liu et al. 2010). Lesion development was examined and recorded as described by Gao et al. (2014a, b), and then photographed using a Nikon D3200 DSLR camera. Each experiment was conducted at least three times.

Results

Identification of cutinase proteins

To identify putative cutinase proteins in the *C. lunata* genome, 34 cutinase proteins from the necrotrophic pathogens *Rhizoctonia solani*, *Phytophthora capsici*, *Fusarium solani*, and *Phaeosphaeria nodorum* SN 15 were used as queries in BLASTP searches for possible homologous cutinase proteins from *C. lunata* using BioEdit® software. As a result,

Table 1 Characteristics of 13 cutinase genes (*ClCUT*) in *Curvularia lunata*

Designated gene name	ORF length (bp)	Amino acid (aa)	Molecular weight (kD)	Isoelectric point (pI)	Location
ClCUT1	651	216	21.6	9.16	Scaffold20
ClCUT2	747	248	25.9	5.54	Scaffold1
ClCUT3	1326	441	40.8	7.61	Scaffold19
ClCUT4	750	249	25.8	8.96	Scaffold4
ClCUT5	714	237	25.1	5.73	Scaffold30
ClCUT6	708	235	23.9	8.31	Scaffold10
ClCUT7	675	224	23.8	7.55	Scaffold30
ClCUT8	1272	423	43.6	5.10	Scaffold15
ClCUT9	996	331	34.1	5.42	Scaffold8
ClCUT10	1071	356	37.1	5.75	Scaffold20
ClCUT11	999	332	33.9	5.48	Scaffold3
ClCUT12	957	318	34.4	6.06	Scaffold1
ClCUT13	402	133	14.7	8.59	Scaffold14

31 candidate proteins from *C. lunata* were obtained that had probability E-value thresholds of 1.0^{-10}. Subsequently, all candidate protein sequences were surveyed using a CDD search in NCBI to further verify whether they contained cutinase domains. Eighteen candidate protein sequences lacked cutinase domains and were discarded. Consequently, 13 non-redundant cutinase proteins were identified and designated as ClCUT1 to ClCUT13. Using ExPASy® tools, we found that the shortest cutinase protein consisted of 133 amino acid residues and the longest had 411 amino acid residues. The respective ORF lengths ranged from 402 to 1326 nucleotides. The predicted molecular weights/isoelectric points of all cutinase proteins ranged from 14.7/9.16 to 40.8/5.10, respectively. All cutinase sequences were distributed on 10 different scaffolds in the *C. lunata* genome (Table 1).

Multiple sequence alignment and intron–exon organization

We conducted a protein sequence alignment among all cutinases from *C. lunata*, 10 cutinase proteins from other plant pathogens, and analyzed some conserved amino acid sites. These data showed that 12 cutinase proteins had highly conserved GYSQG motifs and a DxVCxG[ST]-[LIVMF](3)-x(3)H motif similar to cutinase proteins from other phytopathogens. We also noted that ClCUT13 lacked the conserved GYSQG motif, but contained the DxVCxG[ST]-[LIVMF](3)-x(3)H motif (Fig. 1).

All predicted cutinase genes had different intron–exon patterns in relation to both the position and number of introns, which ranged from 0 to 4 per gene. Based on the number of introns, the cutinases were segregated into four patterns. Pattern1 (*ClCUT3* and *ClCUT8*), pattern 2 (*ClCUT1*, *ClCUT2*, *ClCUT4*, *ClCUT9*, *ClCUT10* and *ClCUT11*), pattern 3 (*ClCUT5*, *ClCUT6* and *ClCUT12*), and pattern 4 (*ClCUT7* and *ClCUT13*) contained 1, 2, 3, and 4 introns, respectively. Furthermore, significant differences in size (41–1326 bp) between the exons were observed. These results showed the different cutinases had variable, complex intron–exon structures (Fig. 2).

Phylogenetic and motif analyses

To examine the relationship between the cutinase genes of *C. lunata* and those from other fungal organisms, we constructed a phylogenetic tree based on the multiple sequence alignment of the 13 ClCUT protein sequences and 78 known cutinases from other fungi. The phylogenetic tree divided these cutinase genes into four groups (Groups 1, 2, 3, 4). Group 1 and Group 3 were further divided into two subgroups (1a and 1b, 3a and 3b), respectively. In our analysis, ClCUT1, ClCUT2 and ClCUT3 were clustered in Group 1a, but ClCUT7 was in Group 1b. ClCUT4, ClCUT5 and ClCUT6 were clustered in Group 2. ClCUT8, ClCUT9, ClCUT11, ClCUT12 and ClCUT13 constituted Group 3a. ClCUT10 was placed in Group 3b as a separate clade. None of the *ClCUT* genes from *C. lunata* were clustered in Group 4. The motif distribution generated by MEME analysis was consistent with the phylogenetic analysis (Fig. 3). Members of the same class shared several of the conserved motifs, which indicated that genes containing these motifs were probably produced from gene expansion within the same class or subclass. For instance, members of Group 1a contained motifs 1, 2, 3 and 10, whereas Group 1b had different motifs. All members of Group 2 contained motifs 1, 2, 3, and 8, whereas Group 3 members contained motifs 2, 4 and 7. It was noted that all *ClCUT* genes had motifs 1, 2 and 3, whereas *ClCUT13* lacked motifs 1 and 3 (Fig. 4). It is likely that *ClCUT13* lost motifs 1 and 3 during evolution. All motifs with characteristic sequences identified by MEME tools are listed in Additional file 6.

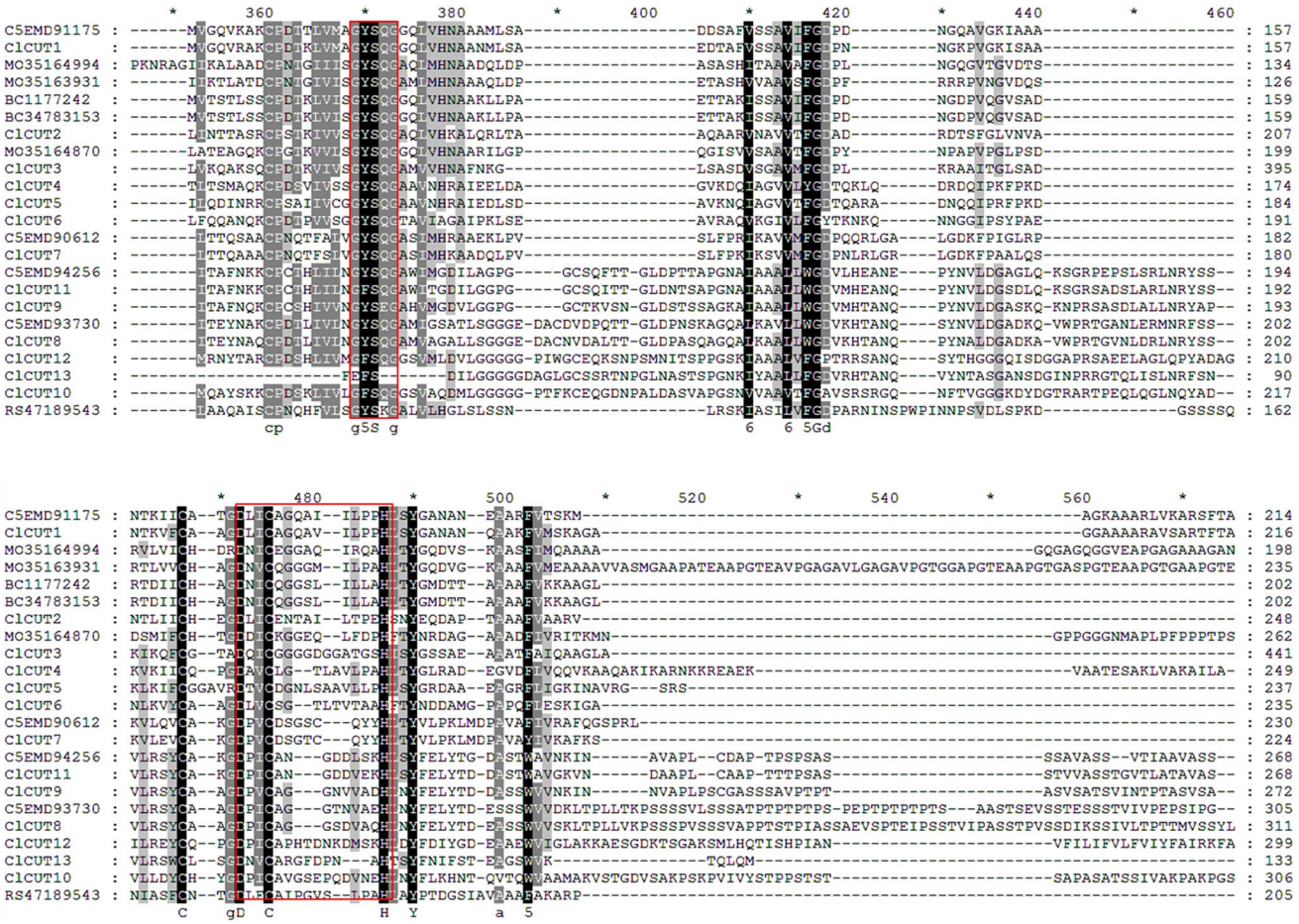

Fig. 1 Multiple sequence alignment of ClCUT proteins in *C. lunata* and 10 known cutinase proteins from different plant pathogens. *Marked with degree of colors* representing for different levels of conservation of each column in the alignment. Two sites with conserved residues are outlined in *red*

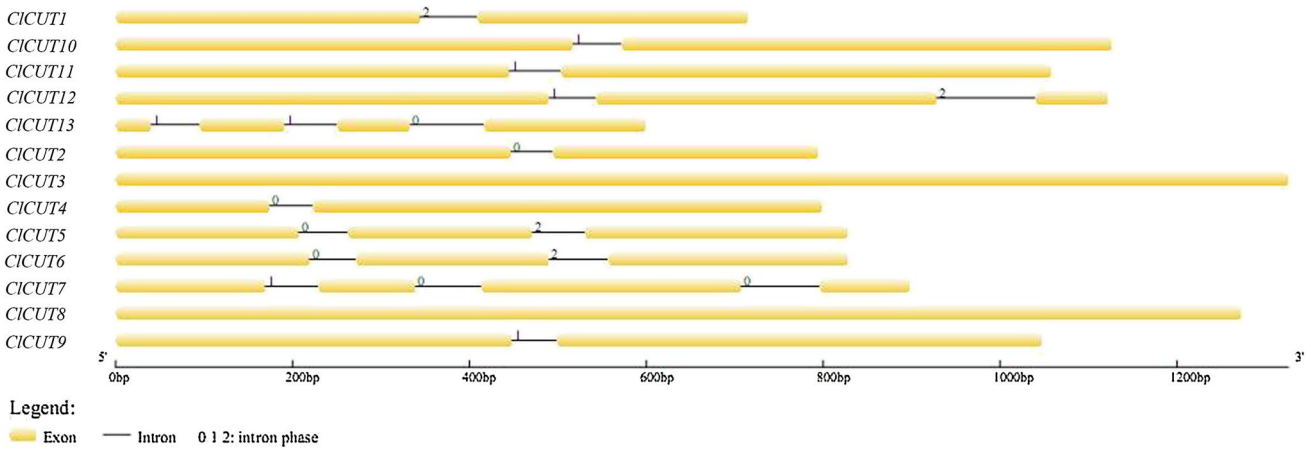

Fig. 2 Intron-exon structures of *ClCUT* genes from *Curvularia lunata*. Exons and introns are indicated by *open boxes* and *lines*, respectively. Different intron types are represented by 0, 1, and 2. The 5′–3′ scale indicates the DNA sequence size. The names of the *ClCUT* genes and intron–exon structures are indicated at the *left* and *right* sides, respectively

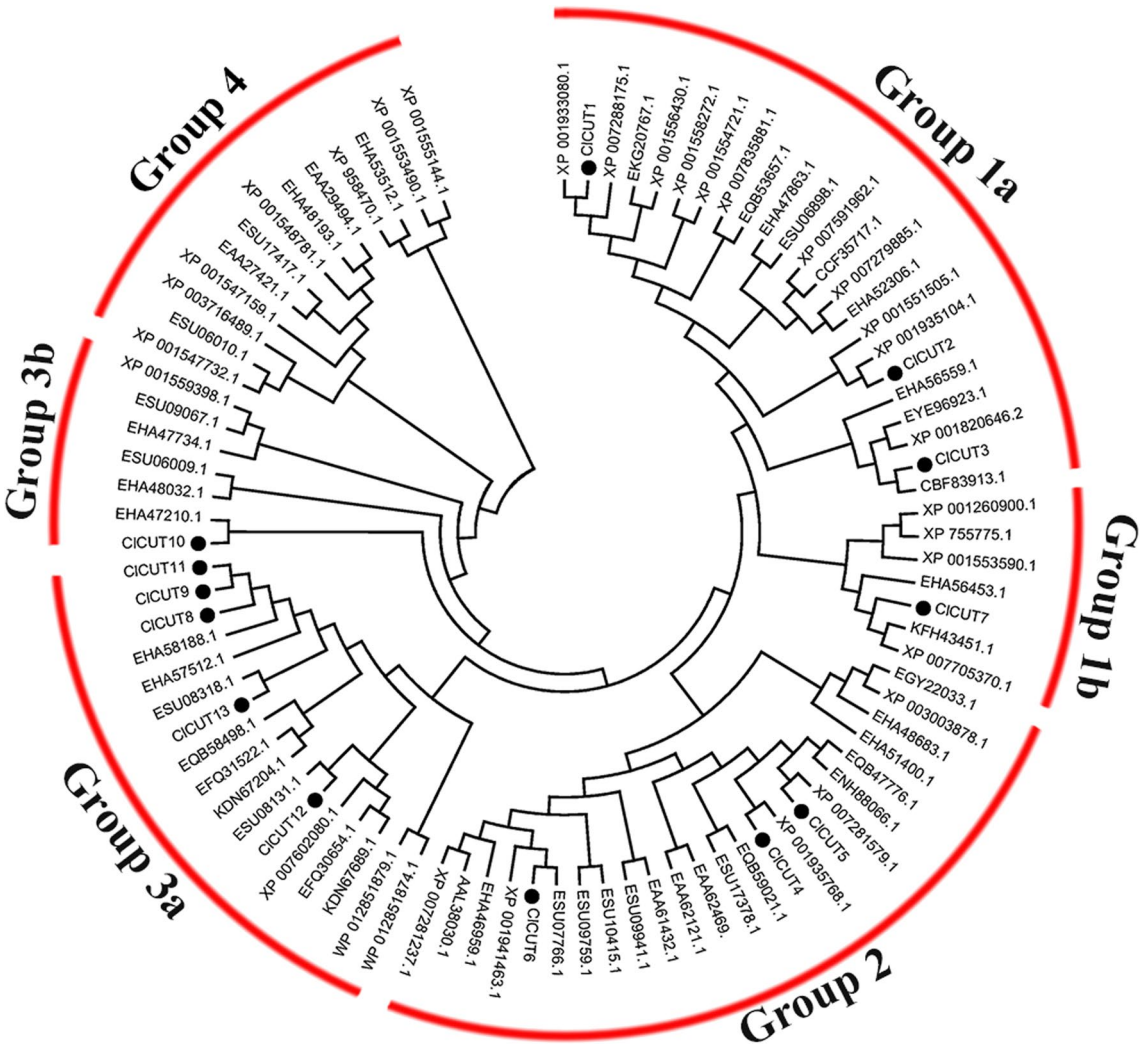

Fig. 3 Unrooted phylogenetic tree representing relationships among ClCUT proteins and cutinase proteins from other plant pathogens. Amino acid sequences of all ClCUT and 78 cutinase proteins were aligned by the Clustal W2 program. The phylogenetic tree was constructed using the neighbor-joining method in MEGA 6.0. The number for each interior branch was the percentage of bootstrap values (1000 replicates). *Black dots* denoted the 13 ClCUT proteins. The *red arcs* indicate different groups or subgroups of cutinase proteins

Expression analysis of cutinase genes

To reveal expression patterns of the cutinase genes during the infection process in maize, we collected leaves at five different times post-inoculation. We then used quantitative-PCR to analyze the cutinase gene expression patterns. Distinct patterns of expression were noted during the compatible interaction between *C. lunata* and maize (Fig. 5). Transcripts of *ClCUT7*, *ClCUT8*, and *ClCUT13* were significantly up-regulated during conidial germination (1.5 hpi) and penetration (3 hpi). The transcript level of *ClCUT7* increased gradually during early infection (0–3 hpi) and reached an eightfold higher expression at 3 hpi compared to conidia at 0 hpi. It then decreased to its lowest level during establishment and colonization at 24 hpi. It is possible that these changes reflect appressorium adhesion and penetration by the pathogen. The transcript levels of *ClCUT8* and *ClCUT13* had a threefold increase in expression during conidial germination (1.5 hpi) and colonization (24 hpi) compared to their levels at 0 hpi. We suggest that *ClCUT8* and *ClCUT13* are not only associated with pathogen penetration, but also colonization. In this study, we also found that the transcript level of *ClCUT6* showed significant up-regulation at 24 hpi compared with other time points. This suggests that *ClCUT6* might have a role in establishment and colonization. In addition, the transcript levels of six cutinase genes (*ClCUT2*, *ClCUT4*, *ClCUT9*, *ClCUT10*, *ClCUT11* and *ClCUT12*) showed little differential expression (<threefold change) at every time point. We therefore considered these genes to be constitutively expressed.

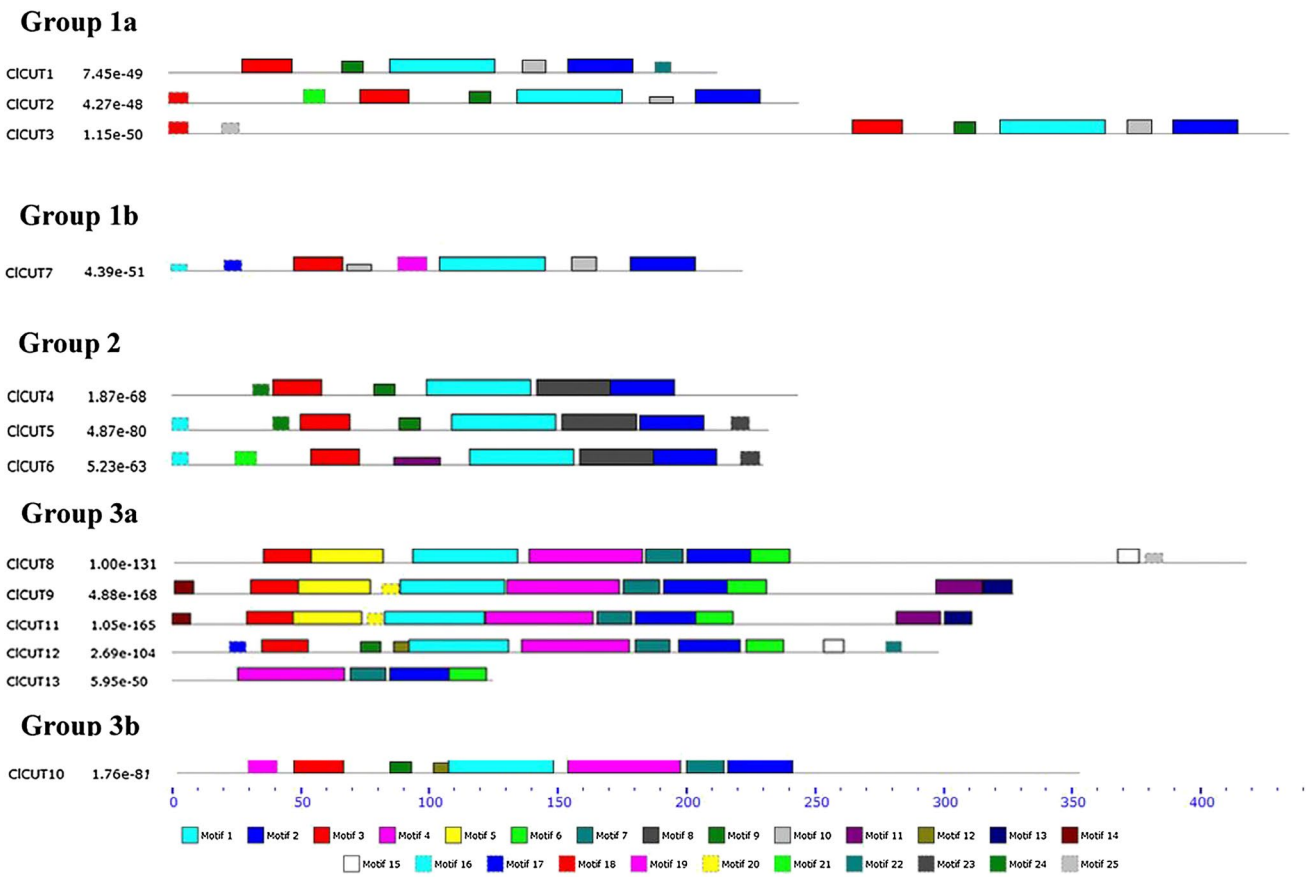

Fig. 4 Schematic diagram of amino acid motifs for all ClCUT proteins from different groups or subgroups. The ClCUT name is listed on the *left*. The *black solid line* represents the corresponding ClCUT protein and its length. The *different-colored boxes* indicate different motifs and their positions in each ClCUT amino acid sequence. A detailed motif sequence characteristic of all ClCUT proteins is shown in the supporting information Fig S1

Deletion and functional analysis of *ClCUT7*

To verify the function of *ClCUT7*, we generated a *ClCUT7* deletion mutant. A 3057-bp deletion cassette containing an 847-bp upstream sequence of *ClCUT7*, 1343 bp of the hygromycin phosphotransferase (*hph*) gene with the TrpC promoter, and 867 bp of the sequence downstream of *ClCUT7* were obtained by double-joint PCR (Fig. 6a). The *ClCUT7* gene was deleted from wild-type *C. lunata* by transformation of *C. lunata* protoplasts with the deletion cassette. Four hygromycin-resistant transformants were selected, and the *hph* gene and *ClCUT7* gene were detected by PCR. The results showed that one transformant had the *hph* gene, but lacked the *ClCUT7* gene, suggesting that this transformant might be a *ClCUT7* gene-disruption mutant. The gene-deletion mutant was confirmed by Southern blotting and RT-PCR and designated ΔClCUT7 (Fig. 6b). The absence of *ClCUT7* mRNA in the ΔClCUT7 transformant was confirmed by RT-PCR (Fig. 6c).

ΔClCUT7 had no obvious changes in phenotype, including colony morphology (Fig. 6d), vegetative growth, conidia production (Table 2), or morphology of the conidia and appressoria (Additional file 7). Three days after inoculation of wounded maize leaves with a conidial suspension, small black lesions were formed at the inoculation sites by both the wild-type strain and ΔClCUT7. The deletion of *ClCUT7* apparently had no effect on the mutant's pathogenicity on wounded leaves compared to the wild-type strain (Fig. 6e; Table 2). However, when unwounded leaves were inoculated with these strains, ΔClCUT7 produced smaller lesions than the wild-type strain, suggesting that the *ClCUT7* deletion had some effect on fungal penetration and resulted in decreased pathogenicity (Fig. 6f; Table 2). To further determine if *ClCUT7* could degrade the cuticle, we cultured the ΔClCUT7 and wild-type strains on media containing either glucose or cutin as a carbon source. Mycelial growth rates for both strains on the medium containing glucose as a carbon source were similar. In contrast, growth of the *ClCUT7* mutant was approximately 10 % slower than the wild-type strain on the medium containing cutin as a carbon source.

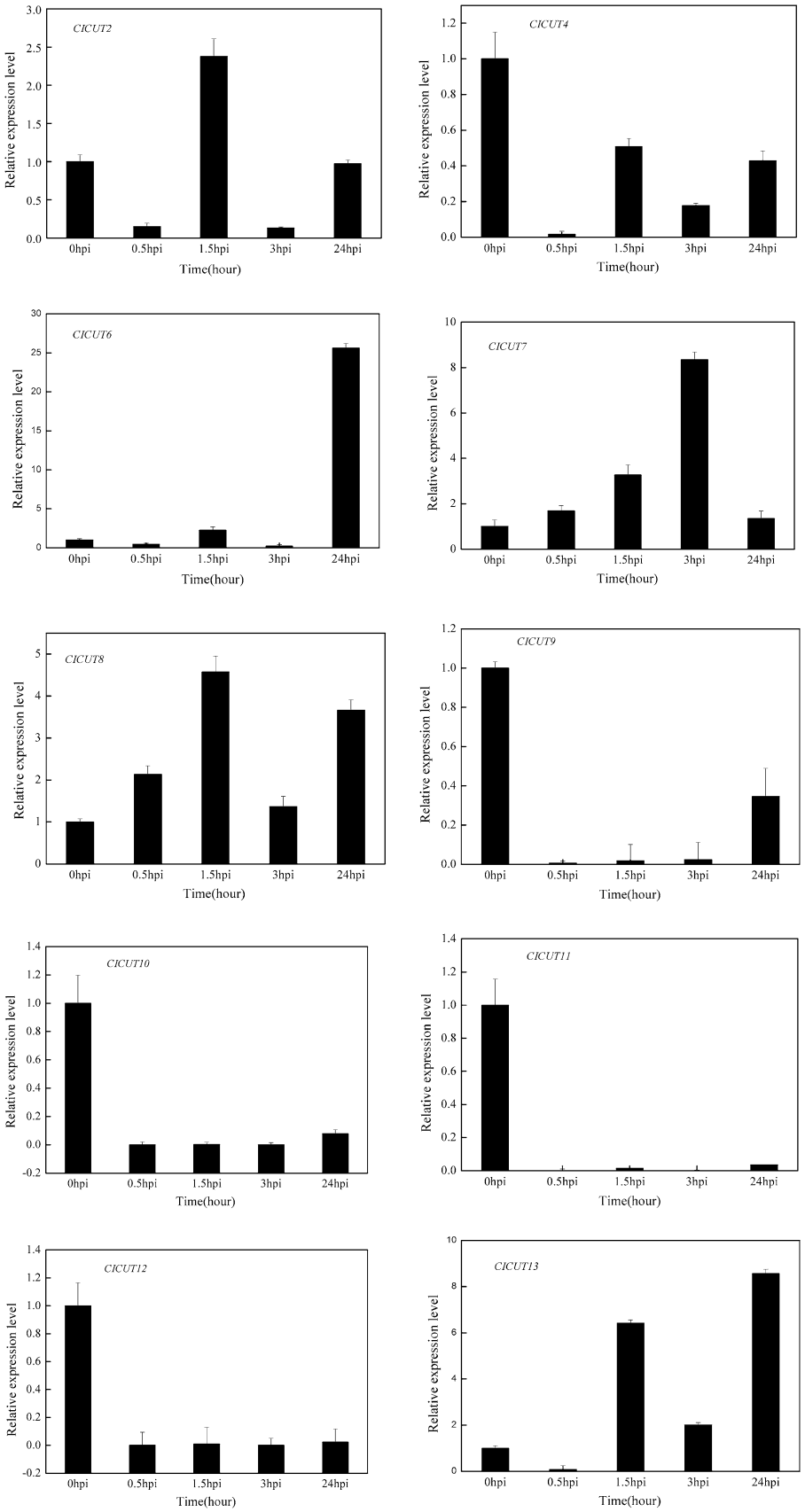

Fig. 5 Expression patterns produced by qRT-PCR of 10 *ClCUT* genes from *C. lunata* during a compatible interaction with maize (*Zea mays*). The relative expression level of mRNA (*y*-axis) was calculated by the comparative C_t method. The *C. lunata GADPH* gene was used as an internal control to normalize the data. Sample time is in hours post-inoculation (*x*-axis). *Error bars* were calculated based on three replicates

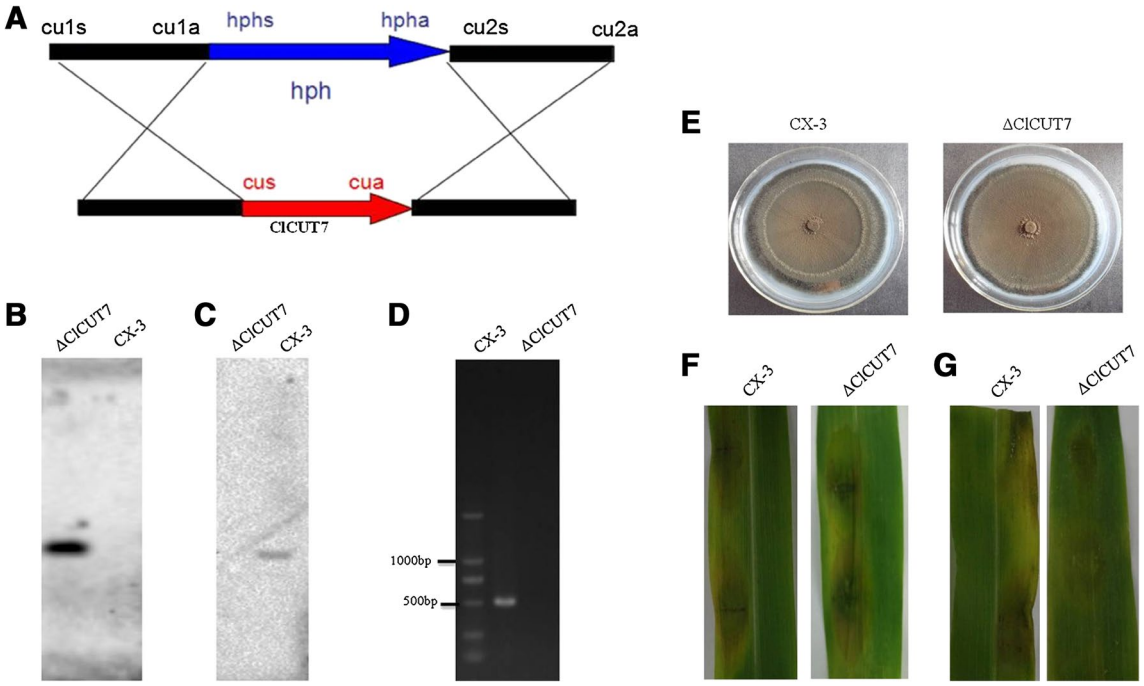

Fig. 6 Construction and confirmation of the *ClCUT7* deletion mutant and functional analysis of the *ClCUT7* gene. **a** Construction of the deletion cassette for *ClCUT7*. *Arrows* indicate orientations of the *ClCUT7* gene (*red*) and hygromycin phosphotransferase (*hph*) gene (*blue*). The deletion cassettes of *ClCUT7* contained homologous sequences flanking the *hph* gene to replace the *ClCUT7* gene ORF. Primer hphs and hpha (Table S5) using amplification of *hph* gene and primer cus and cua (Table S5) using amplification of *ClCUT7* genes were employed to screen the *ClCUT7* deletion mutant. Total of genomic DNA samples isolated from wild-type strain CX-3 and ΔClCUT7 were digested with Page I (**b**) and *Hin*dIII (**c**), then subjected to Southern blot analysis. A hybrid probe, a 610-bp PCR fragment amplified from plasmid pBHt1 with primer hphts (5′-AACTCACCGCGACGTCTGTC-3′) and hphta (5′-TTGTCCGTCAGGAATTGTT-3′) (**b**); A hybrid probe, a 510-bp PCR fragment amplified from the DNA of wild type strain CX-3 with primer JZts (5′-ACCAGCGAGCCCAGTTTC-3′) and JZta (5′-CCTCACCGTTCAAGCATTT-3′) (**c**); **d** total RNA samples from wild-type strain CX-3 and ΔClCUT7 were subjected to RT-PCR using ClCUT7 gene-specific primers cus and cua (Table S5). The RT-PCR product is a 510-bp fragment in the wild-type CX-3 strain as predicted, but is missing in the ΔClCUT7 mutant; **e** colony morphology of the wild-type strain CX-3 and ΔClCUT7 on PDA; **f** disease symptoms on wounded leaves of maize inoculated with conidial suspensions from the wild-type CX-3 strain and the ΔClCUT7 mutant. **g** Unwounded leaves inoculated with the same conidial suspensions. The leaves were photographed 3 days after inoculation

Table 2 Phenotypic analysis of a *Curvularia lunata ClCUT7* gene disruption mutant compared with wild-type strain CX-3

Strain	Growth rate (mm/24 h)	Conidiation ($\log_{10}$ CFU/ml)	Necrotic area on wound leaf (mm^2)	Necrotic area on unwound leaf (mm^2)
CX-3	7.55 ± 0.04a	6.47 ± 0.10a	76.13 ± 2.23a	70.72 ± 0.86a
ΔClCUT7	7.45 ± 0.03a	6.26 ± 0.19a	74.99 ± 0.99a	49.05 ± 1.76b

Data in all columns are the means of three independent experiments with standard deviation. The statistical analysis was performed using the SAS statistical package. Statistically significant analysis of variance was further analyzed using least significant difference tests. Different letters in each column indicate significant differences at $P = 0.05$

Discussion

Previous publications have reported 3 cutinase genes in *Neurospora crassa*, 4 in *Aspergillus nidulans*, 11 in *Botrytis cinerea*, 12 in *Fusarium graminearum*, and 17 in *Magnaporthe grisea* (Skamnioti et al. 2008). In this study, 13 non-redundant cutinase proteins were identified in *C. lunata*. The large number of cutinase genes in *C. lunata* indicated that this fungus produces cutinases that may be able to degrade different types of plant cuticles from various host plants. This may explain the broad host range of *C. lunata*, which includes: sorghum (Akram et al. 2014), lotus (Cui and Sun 2012), rice (Liu et al. 2014), strawberry (Verma and Gupta 2010), spinach (Pandey et al. 2011), zoysia (Roberts and Tredway 2008), and some varieties of turfgrass (Goldring et al. 2007). This pathogen is similar

to *M. grisea,* which produces numerous cutinases able to breach the cuticles of various grasses. Additionally, it has been suggested that a large number of cutinases reflects the need for this enzyme during colonization of the host (Skamnioti et al. 2008).

In this study, 12 of 13 cutinase proteins of *C. lunata* possessed the same amino acid sites (GYSQG). It has been reported that cutinase protein sequences contain a highly conserved motif (GYSQG) surrounding a cutinase-active serine, and a less precise motif (DxVCxG[ST]-[LIVMF](3)-x(3)H) that carries aspartate and histidine residues at the active site (Skamnioti et al. 2008). The amino acid motif GYSQG of the cutinase protein is thought to be crucial for its function. However, when we analyzed intron–exon structures of all 13 cutinase proteins, different and complex intron–exon structures were obtained, suggesting the cutinase genes have undergone ancient and extensive diversification.

C. lunata has an infection process similar to most necrotrophic fungal–plant pathogens. This process includes: host recognition and conidial adhesion; germ tube emergence, elongation, and appressorium formation; host penetration; and establishment in and colonization of plant tissues (Xue et al. 2010). To understand the role of cutinase in the *C. lunata*–maize interaction, we investigated the expression of the pathogen's 13 cutinase genes. Transcript levels of the cutinases quantified by q-PCR indicated that *ClCUT7* was up-regulated early in infection. This suggested that it is associated with cuticle degradation because the cuticle is the first structural obstacle to plant pathogens. Therefore, we examined the role of *ClCUT7* in pathogenicity by knocking out this gene. Additionally, we found that six of the cutinase genes (*ClCUT2*, *ClCUT4*, *ClCUT9*, *ClCUT10*, *ClCUT11* and *ClCUT12*) appeared to be constitutively expressed. Previous research indicated that most of the cutinase genes in *M. oryzae* belonged to constitutively expressed gene groups (Skamnioti et al. 2008). Hence, these cutinase genes may operate synergistically in the interaction between the pathogen and its host plant. The transcript levels of three other cutinase genes (*ClCUT1*, *ClCUT3*, and *ClCUT5*) were not detected in leaf tissue samples, but were detected by quantitative PCR when we used cDNA from pathogen hyphae as templates. It is possible that the expression of *ClCUT1*, *ClCUT3*, and *ClCUT5* was inhibited by the host plant during pathogenesis. Recently, several studies demonstrated that host-induced gene silencing could inhibit the expression of genes in some plant pathogens (Govindarajulu et al. 2014; Ghag et al. 2014). The expression of *ClCUT8* and *ClCUT13* also increased significantly during conidial germination (1.5 hpi) and colonization (24 hpi), respectively. We suggest that both genes may be involved in pathogen penetration and colonization. The specific role of these two genes is being investigated.

Fungal cutinase genes reportedly have different roles in pathogenicity (Dantzing et al. 1986; Kolattukudy 1985; Köller 1991; Sweigard et al. 1992). For example, in *Fusarium solani* f. sp. *pisi*, the presence of cutinases at the site of infection was detected serologically, and the application of chemical cutinase inhibitors prevented fungal penetration (Kolattukudy 1985; Köller 1991). The pathogenicity of cutinase-deficient mutants was reduced but could be restored by adding exogenous cutinases or complementation with the native cutinase gene (Dantzing et al. 1986; Köller et al. 1982). Other studies, however, have provided contradicting evidence about the role of cutinase in pathogenicity (Stahl and Schafer 1992; Stahl et al. 1994). The deletion of the cutinase gene CUT1 of *M. grisea* did not alter the pathogenicity of this fungus on rice (Sweigard et al. 1992). Therefore, the role of cutinase in the plant infection process remains controversial.

C. lunata directly penetrates the cuticle of maize leaves (Mandokhot et al. 1979), suggesting that cutinase played a role in penetration by degrading the cuticle. In our study, deletion of *ClCUT7* had some effect on cuticle degradation, resulting in decreased pathogenicity. This result suggested the cutinases are involved in the pathogenicity of *C. lunata*. Overall, our study characterized the cutinase genes in *C. lunata*, improved our understanding of their expression patterns during compatible interactions with maize, and explored the role of *ClCUT7* in pathogenicity. These findings are a preliminary step in future systematic analyses of cutinase gene functions in *C. lunata*.

Acknowledgments This work was supported by the National Natural Science Foundation of China (Grant Nos. 31272026 and 31301611).

Compliance with ethical standards

Conflict of interest The authors declare no conflict of interest.

Ethical statement This article does not contain any studies with human participants or animals performed by any of the authors.

References

Akram W, Anjum T, Ahmad A, Moeen R (2014) First report of *Curvularia lunata* causing leaf spots on *Sorghum bicolor* from Pakistan. Plant Dis 98:7

Cui RQ, Sun XT (2012) First report of *Curvularia lunata* causing leaf spot on Lotus in China. Plant Dis 96:7

Dai FC, Gao WD, Wu RJ, Jin XH (1995) A noticeable corn disease: curvularia leaf spot. Acta Phytopathol Sinica 25:330

Dai FC, Wang XM, Zhu ZD, Gao WD, Huo NX (1998) Curvularia leaf spot of maize: pathogens and varietal resistance. Acta Phytopathol Sinica 2:123–129

Dantzing AH, Zuckerman SH, Andonov-Roland MM (1986) Isolation of a *Fusarium solani* mutant reduced in cutinase activity and virulence. J Bacteriol 168:911–916

Davies KA, DeLorono I, Foster SJ, Li D, Johnstone K, Ashby AM (2000) Evidence for a role of cutinase in pathogenicity of *Pyrenopeziza brassicae* on brassicas. Physiol Mol Plant Pathol 57:63–75

Dickman MB, Patil SS (1986) A rapid and sensitive plate assay for the detection of cutinase produced by plant pathogenic fungi. Phytopathology 76:473–475

Feng J, Gao ZG, Xue CS, Zhuang JH, Chen J, Bai SY (2002) The pathogenesis of the cell-degrading enzymes produced by *Curvularia lunata*. Rain Fed Crops 22:164–166

Gao JX, Liu T, Li YQ, Chen J (2014a) Insertional mutagenesis and cloning of the gene required for the biosynthesis of the non-host-specific toxin in *Cochliobolus lunatus* that causes maize leaf spot. Phytopathology 104:332–339

Gao SG, Li YQ, Gao JX, Suo YJ, Fu KH, Chen J (2014b) Genome sequence and virulence variation-related transcriptome profiles of *Curvularia lunata*, an important maize pathogenic fungus. BMC Genom 15:627

Ghag SB, Shekhawat UKS, Ganapathi TR (2014) Host-induced post-transcriptional hairpinRNA-mediated gene silencing of vital fungal genes confers efficient resistance against Fusarium wilt in banana. Plant Biotechnol J 12:541–553

Goldring L, Lacasa M, Wright ER (2007) Curvularia Blight on *Lolium perenne* on Turfgrasses in Argentina. Plant Dis 91:3

Govindarajulu M, Epstein L, Wroblewski T, Michelmore RW (2014) Host-induced gene silencing inhibits the biotrophic pathogen causing downy mildew of lettuce. Plant Biotechnol J 16:201–209

Hou JM, Ma BC, Zuo YH, Guo LL, Gao SG, Wang YY, Liu T (2013) Rapid and sensitive detection of *Curvularia lunata* associated with maize leaf spot based on its *Clg2p* gene using semi-nested PCR. Lett Appl Microbiol 56:245–250

Huang XL, Liu LX, Zhai YH, Liu T, Chen J (2008) Proteomic comparison of four maize inbred lines with different levels of resistance to *Curvularia lunata* (Wakker) Boed infection. Prog Nat Sci 19:353–358

Ito MF, Paradela FO, Soave J, Sugimori MH (1979) Leaf spot caused in maize (*Zea mays* L.) by *Curvularia lunata* (Wakker) Boedijn. Summa Phytopathol 5:181–184

Kolattukudy PE (1985) Enzymatic penetration of the plant cuticle by fungal pathogens. Annu Rev Phytopathol 23:223–250

Köller W (1991) The plant cuticle: a barrier to be overcome by fungal plant pathogens. In: Cole GT, Hoch HC (eds) The fungal spore and disease initiation in plants and animals. Plenum press, New York, pp 219–246

Köller W, Allan CR, Kolattukudy PE (1982) Role of cutinase and cell wall degrading enzymes in infection of *Pisum sativum* by *Fusarium solani* f. sp. *pisi*. Physiol Plant Pathol 20:47–60

Li JT, Fu JF, Yan XR, Li HC, Zhou RJ (2006) Analysis of temporal dynamics of Curvularia leaf spot of maize (*Curvularia lunata*) epidemic and yield loss. J Shenyang Agric Univ 6:835–839

Liu T, Liu LX, Hou JM, Li GJ, Gao SG, Chen J (2010) Expression of the green fluorescent protein in *Curvularia lunata* causing maize leaf spot. Can Plant pathol 2:225–228

Liu T, Xu SF, Liu LX, Zhou FH, Hou JM, Chen J (2011) Functional analysis of multi-copy Brn1 gene from the phytopathogenic fungus *Curvularia lunata*. Eur Plant Pathol 131:211–219

Liu LM, Huang SW, Wang L, Hou EQ, Xiao DF (2014) First report of leaf blight of rice caused by *Cochliobolus lunatus* in China. Plant Dis 98:5

Macri F, Lenna P (1974) Leaf corn blight incited by *Curvularia lunata* (Wakk.) Boed. J Plant Pathol 10:27–35

Maddock SE (1979) Studies of the biology of light leaf spot disease of oilseed rape and other brassicas. Ph.D. thesis, University of Cambridge, Cambridge

Mandokhot AM, Singh DP, Chaudhary KCB, Singh JN (1979) Chemical changes in maize leaves in response to leaf spot pathogens. Indian Phytopathol 32:658–660

Pandey RK, Gupta PK, Srivastava M, Singh SR, Gogo R (2011) First report of brown leaf spot disease caused by *Curvularia lunata* infecting Indian spinach or poi (*Basella rubra*). Indian Phytopathol 64:207

Roberts JA, Tredway LP (2008) First Report of Curvularia Blight of Zoysiagrass Caused by *Curvularia lunata* in the United States. Plant Dis 92:1

Shaykh M, Soliday C, Kolattukudy PE (1977) Proof for the production of cutinase by *Fusarium solani* f. *pisi* during penetration into its host, *Pisum sativum*. Plant Physiol 60:170–172

Skamnioti P, Furlong RF, Gurr SJ (2008) Evolutionary history of the ancient cutinase family in five filamentous Ascomycetes reveals differential gene duplications and losses and in *Magnaporthe grisea* shows evidence of sub- and neo-functionalization. New Phytol 180:711–721

Stahl DJ, Schafer W (1992) Cutinase is not required for fungal pathogenicity on pea. Plant Cell 4:621–629

Stahl DJ, Theuerkauf A, Heitefuss R, Schäfer (1994) Cutinase of *Nectria haematococca* (*Fusarium solani* f. sp. *pisi*) is not required for fungal virulence or organ specificity on pea. MPMI 7:713–725

Staitou N, Nei M (1987) The neighbor-joining method: a new method for reconstructing phylogenetic trees. Mol Biol Evol 4:406–425

Sweigard JA, Chumley FG, Valent B (1992) Disruption of a *Magnaporthe grisea* cutinase gene. Mol Gen Genet 232:183–190

Verma VS, Gupta VK (2010) First report of *Curvularia lunata* causing root rot of strawberry in India. Plant Dis 94:4

Xue CS, Zhao ZW, Xiao SQ, Huang WD, Cai L, Chen J (2010) Infection process of *Curvularia lunata* on corn leaf observed in incompatible interaction. J Maize Sci 18:139–141

Yu JH, Hamari Z, Han KH, Seo JA, ReyesDouble- Domínguez Y, Scazzocchio C (2004) Double joint PCR: a PCR-based molecular tool for gene manipulations in filamentous fungi. Fungal genet Boil 41:973–981

Zhang Z, Henderson C, Perfect E, Carver TLW, Thomas BJ, Skamnioti P, Gurr SJ (2005) Of genes and genomes, needles and haystacks: *Blumeria graminis* and functionality. Mol Plant Pathol 6:561–575

Zhou SY, Yang HY, Zhao M, Mei LY (2010) The pathogen identification of maize Curvularia leaf spot and analysis on the enzyme activity of the cell wall-degrading enzyme and lactase. J Maize Sci 5:126–130